EPJ Web of Conferences **308**, 03011 (2024) https://doi.org/10.1051/epjconf/202430803011
ISRD 17

Revision of PSI calculation capabilities and validation experience on the BEPU-type reactor dosimetry applications

Alexander Vasiliev[1,*], *Hakim* Ferroukhi[1], *Marko* Pecchia[1,**], *Dimitri* Rochman[1], *Axel* Laureau[2], *Vincent* Lamirand[2], and *Andreas* Pautz[1,2]

[1]Paul Scherrer Institut, Switzerland
[2]École Polytechnique Fédérale de Lausanne, Switzerland

Abstract. The present paper summarizes the experience accumulated at the Laboratory for Reactor Physics and Thermal-Hydraulics (LRT) of the Paul Scherrer Institute in the field of reactor dosimetry, as well as outlines the recent progress achieved in relation to the associated nuclear data uncertainty propagation methodologies. For dosimetry simulations, the CASMO/SIMULATE/MCNP/FISPACT-II system of codes is in operation at LRT/Nuclear Energy and Safety (NES) Research Division, which is based on the use of validated CASMO/SIMULATE cycle-specific core-follow models of Swiss LWRs. Coupling with FISPACT-II provides the capability for detailed isotopic inventory tracking under irradiation, assessment of materials activation and *dpa* values, etc. The use of the seamless calculation scheme with translation of the core-follow simulation results into the detailed neutron source specifications for consequent Monte Carlo simulations, accomplished with nuclear data uncertainty propagation capabilities and integrated with appropriate dosimetry validation database, makes the PSI methodology well aligned with the generic best estimate plus uncertainty (BEPU) approach principles. For specific illustrations, this paper presents some results on evaluation of: 1) a few well-known OECD/NEA reactor shielding experimental benchmarks (SINBAD benchmarks H.B. Robinson-2, ASPIS-PCA REPLICA), 2) some dosimetry data obtained from a Swiss PWR and 3) simulation of the dosimetry measurements for the 'PETALE' experimental program at the EPFL research reactor 'CROCUS', as they were foreseen at the time of the experimental planning. Finally, ways to further enhance the simulation methodology and models are discussed.

1 Introduction

In the context of the reactor pressure vessel integrity, international and Swiss nuclear reactor safety regulations require determining the 'adjusted reference temperature' (ART), which has acceptable limits for different materials (welds) and zones. A procedure by which ART can be derived is described, for instance, in [1] and it requires as an input parameter, among other

* Corresponding author: alexander.vasiliev@psi.ch
** Current affiliation: Kernkraftwerk Leibstadt AG (KKL)

data, the fast neutron fluence (FNF) for energies E>1MeV and also its attenuation through the reactor pressure vessel (RPV) wall.

Despite the fact that the ART correlation [1] is based on FNF, actually, for the FNF prediction inside the RPV wall, it is recommended to calculate an equivalent FNF attenuation based on the FNF at the RPV inner surface in combination with attenuation of the *dpa* (displacement per atom) inside RPV (in order to appropriately take into account the neutron energy spectrum change within RPV).

Generic attenuation approximations may become non-conservative with increasing distance from the reactor core beltline. Actually, RPV welds and their heat affected zones outside the beltline height may be particularly important since these regions have a higher probability of having flaws. Therefore, high-fidelity BEPU FNF and *dpa* assessments at those locations are more appropriate than simplified evaluations based on generic approximations. Another reason for choosing the BEPU approach is the lack of experimental data for explicit validation of calculations at such important and 'challenging' locations like, for example, BWR core plates or PWR RPV nozzles/welds. Note that since the nuclear data (ND) effects are spectrum-dependent, it is in general important to perform dedicated best-estimate assessments for the particular regions of interest. The combination of codes and tools selected at PSI for LWR dosimetry calculations allows ND uncertainties propagation throughout the entire calculation sequence and for arbitrary quantities of interest. An attention is payed specifically to the ND uncertainties because with accurate modern Monte Carlo codes other important sources of modeling uncertainties, such as related to technological/manufactural parameters, are rather easy quantifiable, provided that information on underlying uncertainty distributions is available (which is in practice often not the case). Some further comments on the calculation uncertainties are provided in Sections 2.1, 3.1 and 4. Also, in the following sections, a general overview of the present status of the LRT/NES/PSI calculation scheme for FNF and ex-core dosimetry/activation assessments, as well as its validation database (benefiting from the NES/PSI Hotlab data), are presented. Afterwards, some recommendations for future methodology and calculation model upgrades are proposed.

2 Current status of the LRT/PSI FNF calculation methodology

2.1 Calculation scheme

A schematic flowchart of the current LRT FNF calculation methodology is illustrated in Fig. 1 and it was discussed in References [2,3].

The "SOURCE4MC" step indicated in Fig. 1 is based on the scripts translating the SIMULATE-3(5) core-follow calculation results into the neutron source data required for the Monte Carlo simulations with the MCNP® code or MCNPX in the past; (see https://mcnp.lanl.gov for details on the MCNP® software trademark). The PSI CMSYS CASMO/SIMULATE models for the Swiss reactors are based on very detailed operation history data, i.e. using tens to hundreds burnup steps per cycle. Thanks to that, the time dependent changes in the spatial-energy source distributions throughout the cycle can be taken into account as accurately as practically needed. Further discussion on this issue is provided in Section 4.

The use of the ADVANTG code [4] for the MCNP variance reduction is very useful for deep penetration neutron transport problems, like, e.g., for concrete bio-shield (including RPV supporting structures) FNF/*dpa*, which should be important for extended reactor life-times justification. The use of the COMPLINK code [5] facilitates coupling of MCNP with FISPACT-II.

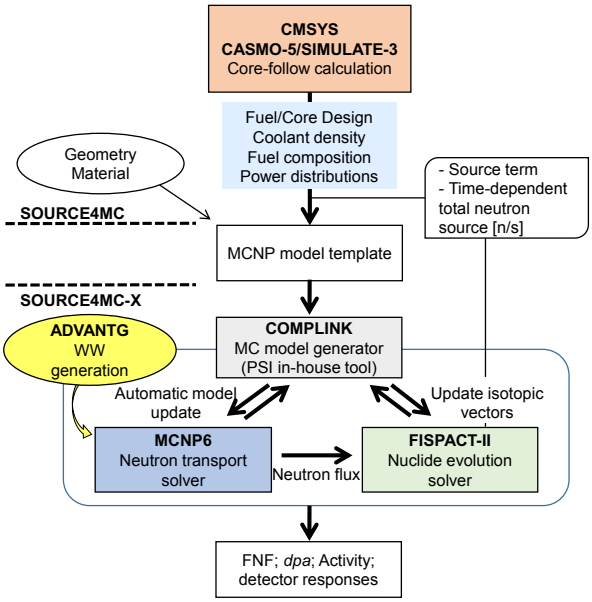

Fig. 1. PSI methodology for LWR structures irradiation & activation evaluations.

It should be outlined that the reference LRT calculation methodology for dosimetry evaluations was not designed for explicit accounting for the 3D pin-wise information on the irradiated fuel composition and respectively the neutron source distributions. A 2D-1D synthesized approach was employed instead for the neutron source strength specifications at each fuel assembly level: 2D radial pin-wise distributions with laterally-averaged 1D axial distributions. The 2D spectrum specifications were based on the FA-average major fissionable nuclides concentrations [2]. Such approach was applied because of the limitations of the reference CMSYS CASMO-4(5)/SIMULATE-3 models and the SIMULATE-3 code itself and clearly constitutes an approximation compared to explicit 3D pin-level distributions in the ideal case. A discussion on this issue improvement is given in Section 4.

To facilitate qualification of the FNF calculation methodology, it has been complemented with the capability for the ND uncertainty quantification (NDUQ) for Monte Carlo simulations using random sampling with the in-house tool NUSS (Nuclear data Uncertainty Stochastic Sampling) [6,7], which is illustrated in Fig. 2. The left top part of Fig. 2 illustrates a covariance matrix with the considered types of ND (non-diagonal yellow blocks indicate presence of covariances, which are nuclear data library (NDL) -specific). The right top part illustrates how a point-wise cross-section and its relative standard deviation look like and the table at the bottom characterizes the NUSS tool in relation to its general methodological features and in comparison with some well-known existing alternative solutions.

On top of that, another in-house tool, SHARK-X (a set of Perl scripts built around the lattice code CASMO5) [6], allows NDUQ at the stage of the CASMO/SIMULATE calculations required for the neutron source specifications. Note that for systematic and comprehensive NDUQ studies, consistent SHARK-X and NUSS cross-section sampling should be realized (i.e. the same perturbation factors should be applied simultaneously in the both tools), as it was recently demonstrated in [6].

Among numerous V&V studies realized at PSI, the most comprehensive are those based on the Swiss reactor experimental data, which allowed validation of the integral calculation sequence based on calculated-to-experimental (C/E) specific activities data, evaluated using calculated reaction rates [8-10]. Details of the realized validation studies are presented further.

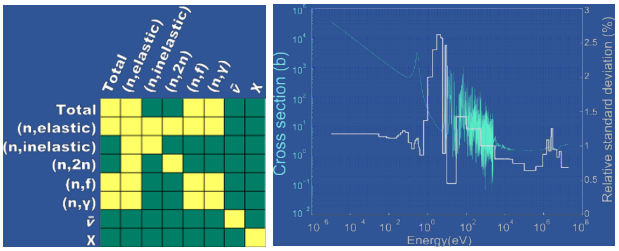

Nuclear data format	Uncertainty format	Global (sampling)	Local (SCS^T)
Basic data	Basic data	TMC	
Evaluated data	Evaluated data	NUDUNA	
Pointwise	Multigroup	NUSS ✓ MCNPX	pert card MCNP6 KSEN McCARD MVP
Multigroup		XSUSA	TSUNAMI-3D MMKKENO

Fig. 2. Highlights on the PSI NUSS stochastic sampling NDUQ capability.

2.2 Validation database

An overview of the experimentally-based reference data used for validation of the PSI methodology is summarized in Table 1. It should be noted that the reported data corresponds to the measurements selected for the PSI validation studies and thus they do not represent the total number of measurements performed at the Swiss reactors and/or concerned experiments (in some cases there could be several measurements which were averaged and considered here as a single reference value). One can see that the LRT/PSI database primarily consists of the data from operational Swiss LWRs and in addition to that, in line with recommendations provided in [1], it includes two well-known and well characterized benchmark models from the OECD/NEA Radiation Shielding and Dosimetry Experiments Database SINBAD.

One of the added values of the SINBAD benchmarks is that they involve dosimetry reactions that are different from those measured for the Swiss reactors. This allows better overall coverage of the incident neutrons energy range of interest (E>1MeV).

The total number of the available C/E values is large enough for efficient statistical assessments, like tolerance interval estimations [12]. In general, it can be a rather sophisticated task to evaluate C/E results. Both the calculated and experimental values are subject of uncertainties, and it is a question how to treat those uncertainties. It is also not a trivial question how to deal with very similar individual experimental measurements. An assessment of similarity of the validation benchmarks and the application case under consideration can be integrated into the C/E results analysis and thus it can influence the conclusions of the methodology qualification, depending on a particular application target. Results of the C/E evaluation for the PWR RPV case are presented below as an illustrative example. Additional discussion is provided in Section 3.1.

Table 1. Summary of the LRT/PSI LWR dosimetry validation database.

Experimental data source	Identification	N. of irrad. cycles	Detectors	C/E sample size
Swiss PWR/ PSI NES Hotlab	RPV Scraping test 1 [2]	21	^{93}Nb(n,n')^{93m}Nb	12
	RPV Scraping test 2 [8], 4 out of 27 elevations not included	27	^{54}Fe(n,p)^{54}Mn; ^{93}Nb(n,n')^{93m}Nb	46 (23 times each det.)
	Barrel irrad. channel, "Gradient Probes" [8]	27	^{54}Fe(n,p)^{54}Mn; ^{93}Nb(n,n')^{93m}Nb	12 (2x3 times each det.)
Swiss BWR/ PSI NES Hotlab	Set 1 Surveillance capsule (to be publ.)	11	^{54}Fe(n,p)^{54}Mn; ^{93}Nb(n,n')^{93m}Nb; ^{63}Cu(n,α)^{60}Co	12 (4 times each det.)
	Set 2 Fluence monitors; RPV cavity [9]	4×1	^{54}Fe(n,p)^{54}Mn; ^{93}Nb(n,n')^{93m}Nb	7 (3 times ^{54}Fe and 4 times ^{93}Nb)
	Set 3 Fluence monitors; RPV cavity [10]	2	^{54}Fe(n,p)^{54}Mn; ^{93}Nb(n,n')^{93m}Nb	2 (1 time each det.)
OECD/ NEA/WPRS SINBAD reactor shielding benchmarks (PWRs)	HBR2-surveillance capsule [11]	9	^{237}Np(n,f)^{137}Cs; ^{238}U(n,f)^{137}Cs; ^{58}Ni(n,p)^{58}Co; ^{54}Fe(n,p)^{54}Mn; ^{46}Ti(n,p)^{46}Sc; ^{63}Cu(n,a)^{60}Co	6 (1 time each det.)
	HBR2- RPV cavity [11]	9	^{237}Np(n,f)^{137}Cs; ^{238}U(n,f)^{137}Cs; ^{58}Ni(n,p)^{58}Co; ^{54}Fe(n,p)^{54}Mn; ^{46}Ti(n,p)^{46}Sc; ^{63}Cu(n,a)^{60}Co	6 (1 time each det.)
	PCA-Replica [13]	NA	^{115}In(n,n')^{115m}In; ^{32}S(n,p)^{32}P	6 (3 times each det.)
Total number of C/E values				**N=109**

3 Application Illustration: PWR RPV FNF

3.1 Validation results analysis

For an illustration, in the following the validation results directly corresponding only to the PWR RPV case are considered (i.e. BWR data is not included), as demonstrated here with Table 2. The validation case nomenclature presents the model type and the dosimeter type. Note that in reality many values labeled with "*i*" in Table 2 are averages obtained for sets of individual measurements (n=*1,…,109*) outlined in Table 1, and for rigorous evaluations the original complete validation database should be used instead of the collapsed data. However, such work goes beyond the scope of this paper. It should be also noted that the values of Table 2 are not fully consistent because for different studies different nuclear data libraries were used so far for neutron transport calculations (reported as "NDL-transport" in Table 2). The dosimeter reaction rates were also calculated with different libraries, including IRDF-2002, but not only. In general, the preference was given to ENDF/B-VII.1 for the sake of consistent usage of the cross-sections and their covariances from the same source, since for the ND uncertainties data, the covariance matrices (CM) of ENDF/B-VII.1 ("E-7.1" in Table 2) were most systematically used [14,15]. The three right hand columns of Table 2 are nuclear data uncertainties. Based on Table 2, the simple average relative difference between the calculated and experimental values, "C/E-1", relevant for an application case response of interest, i.e. FNF at a PWR RPV, equals to -4.7%.

The simplest approach to adjust the future calculation prediction based on the results of the relevant validation studies would be to employ the following correction:

$$R_c^{a*} = R_c^a \cdot 1 \Big/ \left\langle \frac{R_c^b}{R_e^b} \right\rangle , \quad (1)$$

where R_c^a is the calculation result for the application case and the denominator is the average value of the calculated ($R_{c\,i}^b$) to experimental validation benchmark ($R_{e\,i}^b$) response values; i is an individual C/E index.

Table 2. Summary of the LRT/PSI LWR dosimetry validation database.

i	NDL-transport	Validation case	C/E	σ ND-transport, %	σ ND-detector, %	σ ND-total, %
1	E-7.1	PWR_BAR_Fe54	0.993	6.6	2.2	7.0
2	E-7.1	PWR_BAR_Nb93	1.050	7.0	4.4	8.3
3	E-7.1	PWR_RPV_Fe54	1.030	11.0	2.2	11.2
4	E-7.1	PWR_RPV_Nb93	1.034	10.8	4.4	11.7
5	E-7.0	HBR2_Np237	0.938	8.0	1.7	8.2
6	E-7.0	HBR2_U238	0.870	8.0	2.0	8.2
7	E-7.0	HBR2_Ni58	0.885	8.0	1.7	8.2
8	E-7.0	HBR2_Fe54	0.899	8.0	2.1	8.3
9	E-7.0	HBR2_Ti46	0.981	9.0	3.1	9.5
10	E-7.0	HBR2_Cu63	0.862	11.0	2.8	11.4
11	E-7.1	PCA_In115	0.963	7.0	7.2	10.0
12	E-7.1	PCA_S32	0.935	6.0	6.4	8.7

The given "simplified" adjustment is implicitly based on the assumption that the reference values used for validation well represent the application case parameter of interest. In order to justify such assumption, the Pearson correlation coefficient r between the application case and benchmark models' responses can be used, e.g., as concerns the ND effects. Such correlation data is now routinely obtained at LRT using the calculations with ND randomly sampled libraries generated by NUSS, as was illustrated in Fig 2 (varying cross sections and correlating the changes in calculated quantities of interest). Note that hereafter only the ND-related uncertainties and correlations are considered, while in reality there may be other sources of such. For illustration, Fig. 3 shows the correlation coefficients for several calculated values including FNF at the surfaces of the PWR barrel and RPV. The number of calculation parameters is limited in this figure by 20 for better readability.

		PWR_Bar_dpa	PWR_RPV_dpa	**PWR_Bar_FNF**	**PWR_RPV_FNF**	PWR_BAR_Fe54	PWR_BAR_Nb93	PWR_RPV_Fe54	PWR_RPV_Nb93	HBR2_Np237	HBR2_U238	HBR2_Ni58	HBR2_Fe54	HBR2_Ti46	HBR2_Cu63	PCA_In115	PCA_S32	PETALE_Rh103	PETALE_In115	PETALE_Ni58	PETALE_Fe54
		1	2	3	4	5	6	7	8	9	10	11	12	13	14	15	16	17	18	19	20
PWR_Bar_dpa	1	1.00	0.88	0.96	0.86	0.95	0.99	0.76	0.88	0.91	0.87	0.81	0.78	0.57	0.41	0.62	0.60	0.81	0.86	0.86	0.85
PWR_RPV_dpa	2	0.88	1.00	0.84	0.95	0.92	0.88	0.94	0.99	0.88	0.88	0.88	0.86	0.70	0.57	0.79	0.85	0.57	0.59	0.61	0.61
PWR_Bar_FNF	3	0.96	0.84	1.00	0.90	0.87	0.98	0.68	0.87	0.94	0.89	0.74	0.71	0.51	0.37	0.70	0.54	0.73	0.86	0.81	0.79
PWR_RPV_FNF	4	0.86	0.95	0.90	1.00	0.84	0.89	0.85	0.98	0.93	0.91	0.81	0.78	0.63	0.52	0.87	0.78	0.50	0.62	0.58	0.57
PWR_BAR_Fe54	5	0.95	0.92	0.87	0.84	1.00	0.94	0.87	0.90	0.84	0.83	0.87	0.85	0.68	0.52	0.57	0.67	0.76	0.74	0.82	0.83
PWR_BAR_Nb93	6	0.99	0.88	0.98	0.89	0.94	1.00	0.74	0.89	0.93	0.89	0.80	0.77	0.56	0.40	0.66	0.59	0.78	0.86	0.85	0.84
PWR_RPV_Fe54	7	0.76	0.94	0.68	0.85	0.87	0.74	1.00	0.92	0.73	0.76	0.86	0.86	0.80	0.70	0.65	0.83	0.49	0.45	0.53	0.53
PWR_RPV_Nb93	8	0.88	0.99	0.87	0.98	0.90	0.89	0.92	1.00	0.91	0.90	0.86	0.84	0.68	0.56	0.83	0.84	0.54	0.60	0.61	0.60
HBR2_Np237	9	0.91	0.88	0.94	0.93	0.84	0.93	0.73	0.91	1.00	0.98	0.84	0.80	0.60	0.47	0.80	0.67	0.59	0.72	0.70	0.68
HBR2_U238	10	0.87	0.88	0.89	0.91	0.83	0.89	0.76	0.90	0.98	1.00	0.90	0.87	0.68	0.54	0.78	0.71	0.55	0.66	0.67	0.66
HBR2_Ni58	11	0.81	0.88	0.74	0.81	0.87	0.80	0.86	0.86	0.84	0.90	1.00	1.00	0.88	0.74	0.62	0.74	0.57	0.57	0.66	0.66
HBR2_Fe54	12	0.78	0.86	0.71	0.78	0.85	0.77	0.86	0.84	0.80	0.87	1.00	1.00	0.91	0.77	0.58	0.73	0.56	0.55	0.64	0.65
HBR2_Ti46	13	0.57	0.70	0.51	0.63	0.68	0.56	0.80	0.68	0.60	0.68	0.88	0.91	1.00	0.96	0.42	0.60	0.40	0.39	0.47	0.48
HBR2_Cu63	14	0.41	0.57	0.37	0.52	0.52	0.40	0.70	0.56	0.47	0.54	0.74	0.77	0.96	1.00	0.33	0.49	0.26	0.26	0.34	0.34
PCA_In115	15	0.62	0.79	0.70	0.87	0.57	0.66	0.65	0.83	0.80	0.78	0.62	0.58	0.42	0.33	1.00	0.85	0.21	0.35	0.26	0.24
PCA_S32	16	0.60	0.85	0.54	0.78	0.67	0.59	0.83	0.84	0.67	0.71	0.74	0.73	0.60	0.49	0.85	1.00	0.28	0.24	0.27	0.27
PETALE_Rh103	17	0.81	0.57	0.73	0.50	0.76	0.78	0.49	0.54	0.59	0.55	0.57	0.56	0.40	0.26	0.21	0.28	1.00	0.92	0.87	0.86
PETALE_In115	18	0.86	0.59	0.86	0.62	0.74	0.86	0.45	0.60	0.72	0.66	0.57	0.55	0.39	0.26	0.35	0.24	0.92	1.00	0.89	0.87
PETALE_Ni58	19	0.86	0.61	0.81	0.58	0.82	0.85	0.53	0.61	0.70	0.67	0.66	0.64	0.47	0.34	0.26	0.27	0.87	0.89	1.00	1.00
PETALE_Fe54	20	0.85	0.61	0.79	0.57	0.83	0.84	0.53	0.60	0.68	0.66	0.66	0.65	0.48	0.34	0.24	0.27	0.86	0.87	1.00	1.00

Fig. 3. ND-related Pearson correlation coefficients for the selected quantities of interest.

From the obtained data it should be seen, for example, which C/E results are more appropriate for validation of, e.g., the FNF predictions at PWR RPV. Obviously, the experimental data corresponding to the RPV scraping tests or to the HBR2 fission dosimeters are very appropriate for this target. Naturally, Fig. 3 also confirms high correlations between the FNF and *dpa* calculation results. Finally, apart from the existing validation data indicated in Table 2, Fig. 3 illustrates the correlations between the considered parameters of interest and the measurements which were foreseen for the PETALE experimental program at the EPFL CROCUS reactor, at the time of the initial experimental planning (in 2019). Such information provides a qualitative assessment of applicability of the expected PETALE experimental data for validation of practical LWR dosimetry predictions.

There exist more sophisticated validation procedures that can be applied for the dosimetry evaluations, based on the Bayesian inference. It should be recalled that for rigorous Bayesian framework application one needs to know not only the ND-related uncertainties and correlations like those reported above, but also other types of covariances such as related to design manufactural/technological tolerances and related to measurement techniques. For instance, some experimental data corresponding to the "E" parameters reported in Table 2 shall be highly correlated, e.g., when corresponding to the same reactor and measurements locations (e.g., if different fluence monitors share the same uncertainties of their positions); the specific activity measured data can share the same methodological uncertainties (can be done with similar/same measurement and evaluation techniques and even using the same instrumentation), etc. The calculated parameters "C" in Table 2, in addition to the ND-related uncertainties, can share the uncertainties in the neutron source specifications (related to the methodology, design and operating history information, etc.). It is a very complicated task, however, to make estimations of such data in practice. Another obstacle can be related to the potential (self-)inconsistency or incompleteness of the modern NDL CM (under concern are, for instance, the total (MT-452 in ENDF-6 format) and prompt (MT-456) nu-bar covariance data in ENDF/B-VII.1 [16] and the angular scattering distributions outlined in Section 4), however such discussion goes beyond the scope of the paper.

The easiest way of using the ND- related correlations is to focus on those benchmarks that have highest correlations with application cases. For instance, following some "common rule of thumb", one can set the cut-off value† for *r* by 0.8. If the average C/E-1 value is now recalculated using Table 2 data only for the cases where *r*>0.8, it becomes -3.0%. In the given example, the relative difference between the two C/E-1 results (taking and not taking into account the *r* cut-off) is ~36%, and in general it is case-specific.

Another relevant value that depends on the *r* cut-off is the uncertainty of R_c^{a*}, which can be easily assessed with random ND sets, as can be realized with, e.g., NUSS. In the case of high correlations between R_c^a and $\langle \frac{R_c^b}{R_e^b} \rangle$ the resulting variance of R_c^{a*} will be much smaller compared to the simple sum of variances of R_c^a and $\langle \frac{R_c^b}{R_e^b} \rangle$, thanks to the correlation-induced cancellation effect, according to the error propagation formula for a ratio of random values (note that R_e^b is not supposed to have the ND-related uncertainty). An illustration of similar effects was shown, for instance, using the same NUSS-based calculations, but for the case of criticality safety validation studies [17].

† Reduced C/E sample size can affect the statistical evaluations, e.g. lead to increased tolerance intervals, etc.

3.2 PWR RPV FNF assessment

In relation to the issue on generic attenuation approximations outlined in the Introduction, as an illustration, a practical application of the LRT/PSI calculation scheme is described here. Fig. 4 shows the FNF and *dpa* calculated results for a Swiss PWR RPV.

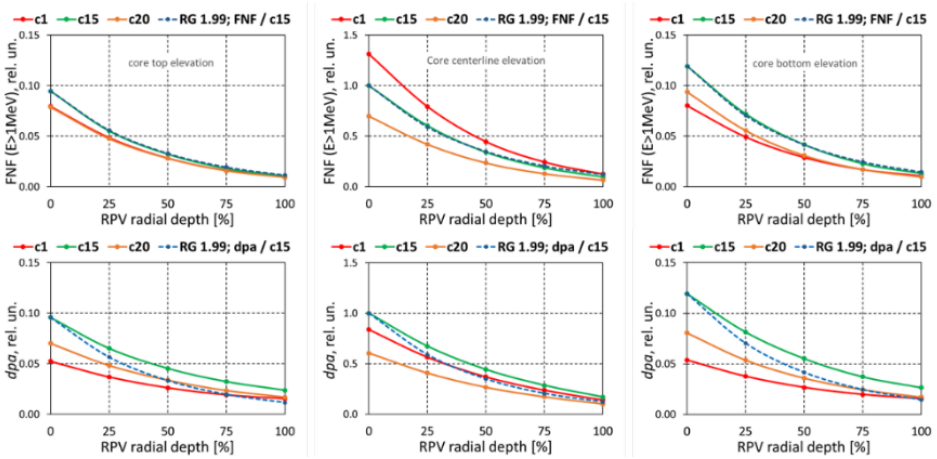

Fig. 4. FNF and *dpa* attenuation inside the PWR RPV wall for selected reactor cycles; normalized.

The results correspond to three different axial elevations at RPV: at the level corresponding to the top end of the fuel assembly active part, at the core centerline and at the bottom of the fuel assembly active part. As well, results are shown for average conditions at three different reactor cycles: cycles 1, 15 and 20. It is relevant to mention that at cycle 1 the "out-in-in" fuel management scheme was employed, at cycle 15 there was the "partial low-leakage" scheme in place, while by cycle 20 the "low-leakage" scheme was finally established, which helped to reduce the FNF exposure at RPV [18]. One can notice an excellent agreement of the correlation conventionally used for the estimation of the inside-wall FNF attenuation, as provided in US NRC Regulatory Guide 1.99, with the detailed calculation results at different axial elevation of RPV. Referring to the *dpa* attenuation discussed in the Introduction, it can be confirmed that the generic RG 1.99 correlation does not agree well with it (as the attenuation equation was developed for fast neutron flux and not for *dpa*), especially at the axial elevations at the top and bottom of the RPV beltline (core axial boundaries).

4 Towards the calculation scheme and models further upgrading

The PSI calculation scheme was initially oriented on the use of the SIMULATE-3 code and available at the time CMSYS models, which did not directly provide 3D pin-power distributions, as was explained in Section 2.1. The transition from SIMULATE-3 to SIMULATE5 (see for reference https://www.studsvik.com/key-offerings/nuclear-simulation-software/software-products/simulate5/) is already on-going at LRT/PSI and the advantages of SIMULATE5 methods (e.g. as concerns the 3D pin power distributions), together with refining the PSI models for producing detailed pin-wise outputs, shall allow improvement of the neutron source strength specifications.

Furthermore, another code of the Studsvik CMS codes family, 'SNF' (the code for 3D spent nuclear fuel characterization and analysis, see https://www.studsvik.com/key-offerings/nuclear-simulation-software/software-products/snf/), has been preliminary integrated at LRT within the CMSYS system of models for the Swiss reactors. The use of

SNF allows the extraction of detailed results on the burned nuclear fuel distributions and consequently can help with producing explicit 3D pin-wise neutron source strength and spectrum specifications. This advantage was implemented in the new PSI "CS2M" methodology [19], originally oriented towards criticality applications. Those recent developments have enabled further improvements of other down-stream calculations, like for LWR dosimetry applications. Thus, it can be proposed to integrate now the CS2M capabilities into the CASMO/SIMULATE/MCNP+FISPACT computational scheme, for advancing BEPU dosimetry and activation calculations.

Another important upgrade can be done on the side of NDUQ, with respect to the uncertainty propagation for the differential scattering cross-sections/scattered neutron angular distributions. It was found that the uncertainties of such distributions can be very important contributors to the overall calculation of uncertainties and especially the influence of ^{16}O elastic scattering was outlined [20]. In particular, it was shown that for PWR RPV assessments just the differences between the JENDL-4.0 and ENDF/B-VII.1 libraries for the angular distributions of ^{16}O(n,n) lead to the differences in RPV FNF of ~10% for the PWR and ~20% for the BWR cases. For comparison, typical levels of uncertainties of FNF at RPV inner surface, associated with uncertainties of all other ND except the angular distributions, were found around ~10% for the PWR (see also Table 2) and ~15% for the BWR reactors [15]. Unfortunately, even with the recent release of the latest ENDF/B-VIII.0 library, the information on uncertainties of such data is not yet complete. For further illustration, Fig. 5 presents the relative uncertainties of the mu-bar data specified in JENDL-4.0 and ENDF/B-VIII.0, together with the relative mu-bar differences between the two libraries.

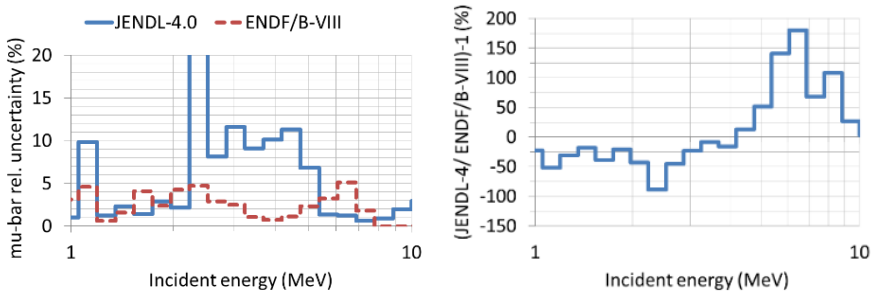

Fig. 5. Information from the modern NDLs; left - mu-bar uncertainties; right – ration of the mu-bars.

One can see that the uncertainty information is inconsistent with the observed data differences. Note that so far only the mu-bar uncertainties are provided in the modern NDLs, while in theory more detailed (i.e. for higher than the first order Legendre coefficient, which is the average scattering angle or mu-bar) information is needed. Thus, when they finally become available, the angular scattering distributions' uncertainties will be necessary to include into the overall NDUQ assessments, in order to correctly estimate not only the ND-related uncertainties, but also the related correlations between the considered quantities of interests, as those shown in Section 3.1 of this paper.

It should be also mentioned that in certain cases, especially for BWRs, a proper accounting for variations of the operating conditions and related neutron source (re)distributions can be quite important for dosimetry assessments. As an example, Fig. 6 shows the relative power fraction (RPF) variation for an axial node of a peripheral FA, which provided the most significant contribution to the response of one of the FNF monitors during the first operating cycle of a Swiss BWR. Naturally, subdivision of the entire cycle irradiation history into shorter time/BU steps (e.g., on the monthly basis, in line with industry standard practices) allows more accurate dosimetry assessments.

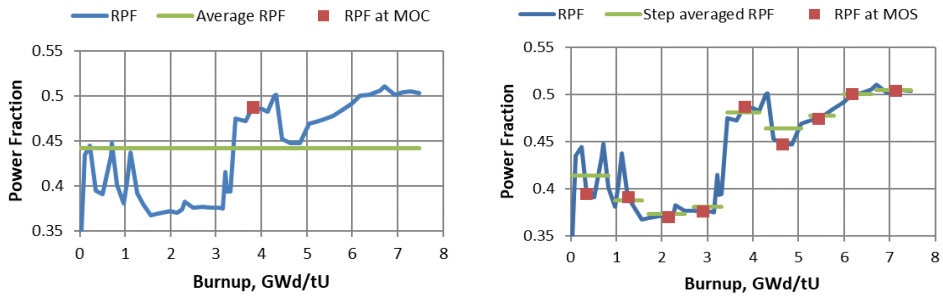

Fig. 6. Illustration on the BU-dependent RPF behavior in comparison with Middle-of-Cycle (MOC) RPF, cycle-average RPF and several Middle-of-Step (MOS) RPF values.

So far, the number of time/BU steps for dosimetry simulations have been arbitrary selected by the modelers, on an educated guess basis. Thus, it would be useful to upgrade in the future the LRT FNF methodology with a unified automated procedure for optimized step-wise representation of the operating history and the neutron source in the MCNP models. Some developments and sensitivity studies towards such improvements were reported in [7,11].

Finally, it should be noted that for BEPU RPV FNF assessments it is also important to know the coolant density/temperature in the core bypass region, which can be done with dedicated CFD simulations, as was preliminary illustrated in [21].

5 Conclusions

This paper briefly summarizes the status of the calculation methodology established at LRT/NES/PSI for LWR dosimetry applications and its validation basis which primary consists of data from experimental programs realized at Swiss PWR and BWR reactors and at PSI Hotlab. In addition, the HBR-2 and ASPIS-PCA REPLICA benchmarks from the OECD/NEA SINBAD database were also included in the PSI validation suit.

The current research interest at LRT is to foster the capabilities for the dosimetry assessments beyond RPV and beltline regions, which become important for safe long-term LWRs operation. Such enhancements should be realized in combination with certain methodology and modeling upgrading as indicated in this work, namely on the neutron source specifications refinement, uncertainties quantification advancement and automation of the calculation models development.

In parallel, a further extension of the validation database is foreseen, e.g. by addition of the SINBAD VENUS-3 and Balakovo-3 benchmarks, as well as new experiments at the EPFL CROCUS research reactor.

Finally, a special attention should be paid to review of the available experimental data quality and to verification if all relevant phenomena were properly taken onto account in the C/E results evaluation (e.g., if all nuclear reactions leading to production of the measured radioactive isotopes were properly accounted for).

The authors are grateful to the anonymous reviewers for their very thorough and constructive reviews. The first author would like to express his sincere gratitude to Dr. Roberto Capote and Prof. Dr. dr. h. c. Hamid Aït Abderrahim for valuable comments to this work provided at the ISRD17 Symposium.

References

1. U.S. Nuclear Regulatory Commission, Regulatory Guide 1.99, Radiation Embrittlement of Reactor Vessel Materials, Revision 2
2. A. Vasiliev, H. Ferroukhi, M.A. Zimmermann, R. Chawla, Ann. Nucl. Energy **34(8)**, 615 (2007)
3. A. Vasiliev, M. Pecchia, D. Rochman, H. Ferroukhi, EPJ Web Conf. **247**, 10021 (2021)
4. S. W. Mosher, S. R. Johnson, A. M. Bevill, A. M. Ibrahim, C. R. Daily, T. M. Evans, J.C. Wagner, J. O. Johnson and R. E. Grove, ORNL/TM-2013/416 Rev. 1, Oak Ridge National Laboratory, Oak Ridge, TN, USA (2015)
5. M. Pecchia, J. J. Herrero, H. Ferroukhi, A. Vasiliev, S. Canepa, A. Pautz, *Int. Conf. Nuclear Criticality Safety, ICNC 2015*, Charlotte, NC, USA, September 13-17 (2015)
6. M. Frankl, M. Hursin, D. Rochman, A. Vasiliev, H. Ferroukhi, Appl. Sci., **11(14)**, 6499 (2021)
7. A. Vasiliev, D. Rochman, M. Pecchia, H. Ferroukhi, Energies **9, 1039**, 1 (2016)
8. A. Dupré, A. Vasiliev, H. Ferroukhi, A. Pautz, Ann. Nucl. Energy **85**, 820 (2015)
9. A. Vasiliev, W. Wieselquist, H. Ferroukhi, S. Canepa, J. Heldt, G. Ledergerber, Progress in Nuclear Science and Technology, **4**, 99 (2014)
10. A. Vasiliev, W. Wieselquist, H. Ferroukhi and S. Canepa, *Int. Conf. M&C2011*, Rio de Janeiro, Brazil, May 8-12, 2011 (2011)
11. R. Pittarello, A. Vasiliev, H. Ferroukhi, R. Chawla, Ann. Nucl. Energy, **38**, 1842 (2011)
12. H. Lee, A. Vasiliev, H. Ferroukhi, Ann. Nucl. Energy **181,** 109556 (2023)
13. A. Vasiliev, M. Pecchia, D. Rochman, G. Perret, H. Ferroukhi, A. Laureau, V. Lamirand, and A. Pautz, EPJ Web Conf. **239**, 22001 (2020)
14. A. Vasiliev, M. Pecchia, D. Rochman, H. Ferroukhi, *Int. Conf. PHYSOR 2020*, Cambridge, UK, March 29 - April 2 (2020)
15. A. Vasiliev, M. Pecchia, D. Rochman, H. Ferroukhi, E. Alhassan, EPJ Web Conf. **239**, 22003 (2020)
16. D. Rochman, A. Vasiliev, H. Ferroukhi, T. Zhu, S.C. van der Marck, A.J. Koning, Ann. Nucl. Energy **92**, 150 (2016)
17. A. Vasiliev, D. Rochman, M. Pecchia, H. Ferroukhi, Ann. Nucl. Energy, **116**, 57 (2018)
18. A. Vasiliev, H. Ferroukhi, E. Kolbe, M.A. Zimmermann, *Int. Conf. PHYSOR'08*, Interlaken, Switzerland, September 14-19 (2008)
19. D. Rochman, A. Vasiliev, H. Ferroukhi, M. Pecchia, J. Hazard. Mater. **357,** 384 (2018)
20. A. Vasiliev, D. Rochman, M. Pecchia, H. Ferroukhi, *Int. Conf. PHYSOR 2018*, Cancun, Mexico, April 22-26 (2018)
21. I. Clifford, M. Pecchia, R. Puragliesi, A. Vasiliev, H. Ferroukhi, Nucl. Eng. Des., **330** 117 (2018)